Biomimetic Approach to the Formation of Titanium Dioxide Thin Films by Using Poly(2-(dimethylamino)ethyl methacrylate)

Sung Ho Yang, Kyungtae Kang, and Insung S. Choi*[a]

Abstract: We demonstrate that the biomimetic method—which has been used for the formation of silica thin films—also could be applied directly to the formation of titanium dioxide (TiO_2) thin films, which are technologically important materials because of their applications to photocatalytic purifiers, photochemical solar cells, and others. After generation of poly(2-(dimethylamino)ethyl methacrylate) (PDMAEMA) films on gold surfaces by surface-initiated polymerization, titanium bis(ammonium lactato)dihydroxide was used as a precursor of TiO_2. The TiO_2/PDMAEMA films were successfully formed on the surfaces in aqueous solution at neutral pH (pH 6.7) and room temperature, and were characterized by X-ray photoelectron spectroscopy, Fourier transform infrared spectroscopy, atomic force microscopy, scanning electron microscopy, and X-ray diffractometry. The formed TiO_2 films have an amorphous nature and large area uniformity in thickness. The degree of crystallization was controlled by annealing. We also investigated the pH effect and the phosphate incorporation in the films by using phosphate-buffered solutions. The TiO_2 films were formed in all the employed pH values in the range of 2 to 12, but phosphate anions were found to be incorporated into the films facilely only at low pH.

Keywords: biomineralization · biosilicification · biomimetic synthesis · thin film · titanium dioxide

Introduction

While many inorganic materials are often synthesized chemically under extreme temperature and pressure,[1,2] the biological formation of inorganic minerals found in nature (biomineralization) occurs under ambient conditions in aqueous solutions.[3] Biomineralization has recently drawn a great deal of interest in the field of materials sciences, as a potential alternative to the chemical method requiring harsh reaction conditions.[4,5] The approach of biomimetic mineralization has successfully been applied to the formation of various nanostructured biominerals, such as calcium carbonate, calcium phosphate, silica, and iron oxide.[6–10] In addition, fundamental studies of biomineralization processes themselves have led to the biomimetic synthesis of abiological materials.[11–19] For example, ferritin, an iron oxide-producing protein,[10] has been used to form abiological inorganic materials, such as oxohydroxides of cobalt, manganese, and nickel, under physiological conditions.[11–13] Silicateins, silica-forming proteins,[20] have also been used for forming titanium dioxide and gallium oxide.[14,15]

Among various biominerals, silica, the second most abundant biomineral, has been studied intensively, because not only does biosilicification (found in diatoms[21] and glass sponges[22]) occur under ambient conditions at slightly acidic pH values, but the formed silica structures are also precisely controlled at the nanometer scale. Biosilicification in diatoms is reported to be achieved by specific interactions between silicic acid derivatives and biopolymers, such as cationic peptides named silaffins.[23] Silaffins are posttranslationally modified peptides, where many lysine residues are modified to ε-*N*-dimethyllysines or oligo-*N*-methylpropyleneimine-linked lysine residues, and serine residues are modified to phosphorylated serine residues. The self-assembled structure of the peptides is thought to act as a template for in vivo polycondensation of silicic acid derivatives catalyzed by the long-chain polyamines in diatoms.[24–28] It is also suggested that the self-assembly of the peptides is mediated by electrostatic interactions between cationic long-chain polyamines and phosphate anions in silaffins.[29,30]

Based on the aforementioned finding, silica nanospheres have been synthesized biomimetically in vitro with various

[a] S. H. Yang, K. Kang, Prof. Dr. I. S. Choi
Department of Chemistry and School of Molecular Science (BK21), KAIST
Daejeon 305-701 (Korea)
Fax: (+82) 42-350-2810
E-mail: ischoi@kaist.ac.kr

polyamines, such as poly-L-lysine,[31] poly-L-histidine,[32] poly-L-arginine,[33] poly(allylamine hydrochloride),[26,34,35] amine-terminated dendrimers (PPI and PAMAM),[36,37] and others.[38,39] In addition to the nanospheres, we for the first time reported the formation of silica thin films with poly(2-(dimethylamino)ethyl methacrylate) (PDMAEMA) as a synthetic counterpart of silaffins, based on the fact that most of the amines in silaffins are tertiary.[40,41] Several abiological materials also have been synthesized based on the proposed mechanism of biosilicification in diatoms. Clarson et al. have shown that microparticles of amorphous germanium oxide could be formed at neutral pH by using poly(allylamine hydrochloride) and poly-L-lysine as synthetic counterparts of silaffins.[16] Naik et al. have demonstrated the formation of titanium oxide-coated, single-walled carbon nanotubes by using a bifunctional fusion peptide (P1R5) composed of a single-walled carbon nanotube-binding part (P1) and inorganic-precipitating part (R5).[42] Wright et al. have produced TiO_2 nanoparticles with R5 peptide and poly-L-lysine under ambient conditions,[43] and Kröger et al. have synthesized TiO_2 crystals with recombinant silaffins.[44,45] A series of the previous reports indicate that the very same process of biomimetic silica formation, utilizing amine-containing polymers as a catalytic template, can be applied directly to the synthesis of various abiological metal oxides under ambient conditions.

Among the abiological inorganic materials synthesized by the biomimetic approach, TiO_2 is one of the highly important materials because of its applications to photocatalytic purifiers,[46] photochemical solar cells,[47,48] and others. For the high functional efficiency of TiO_2-based materials, TiO_2 is generally formed as thin films, and the TiO_2 thin films have been prepared by various techniques, including evaporation,[49] chemical vapor deposition,[50,51] sputtering deposition,[52–55] ion beam-assisted processes,[56] and sol–gel processes.[57] While successful, these techniques generally need heterogeneous conditions that require high temperatures and pressures as well as caustic chemicals.[58–60] In addition, the uniformity of the thickness over a large area is relatively poor. As an alternative, a solution-based approach for depositing TiO_2 films onto surfaces has been attempted. Self-assembled monolayers (SAMs) terminating in sulfonate or hydroxyl groups were formed on Si/SiO_2 to control surface functionality, and TiO_2 films were grown on the surfaces with either highly acidic titanium tetrachloride[61] or anhydrous titanium isopropoxide[62] as a precursor. Micropatterns of TiO_2 films also have been generated on the patterned SAMs by the solution-based deposition method.[63] Baskaran et al. reported the deposition of relatively uniform TiO_2 films under mild deposition conditions by using titanium bis(ammonium lactato)dihydroxide (TBALDH) as a precursor: The control of TiO_2 deposition on surfaces was achieved by using acid decomposition of TBALDH at 70 °C.[64] To the best of our knowledge, there has been no report on the use of silaffins or their synthetic substitutes for the biomimetic formation of TiO_2 films.

We reasoned that our previously reported method for forming silica thin films could be applied to the formation of TiO_2 thin films under ambient conditions (i.e., neutral pH and room temperature); in this work, we used films of PDMAEMA and quaternized PDMAEMA,[40,41,65] which we had used for the formation of silica thin films, as biomimetic templates for the formation of TiO_2 thin films. As a precursor for TiO_2, TBALDH was employed, because this compound has successfully served as a TiO_2 source in previous reports.[14,42–44,64] Because it was reported that a TiO_2 film was not formed from TBALDH in solution at neutral pH and ambient temperature in the absence of amine-based catalytic templates,[44] we believed that TBALDH would be a suitable candidate for investigating biomimetic formation of TiO_2 films with PDMAEMA and quaternized PDMAEMA as catalytic platforms. The formed TiO_2 films were characterized by Fourier transform infrared spectroscopy, X-ray photoelectron spectroscopy, atomic force microscopy, scanning electron microscopy, and X-ray diffractometry.

Results and Discussion

As mentioned above, the biosilicification in diatoms is achieved by specific interactions between cationic silaffins and silicic acid derivatives. Silaffins contain long-chain polyamines composed of methylated tertiary and quaternary amines. Previously, we biomimetically produced silica thin films and their micropatterns with a tertiary amine-containing polymer, PDMAEMA.[40,41] In addition, we also reported the formation of superhydrophobic surfaces based on the biomimetic silicification with quaternized PDMAEMA (q-PDMAEMA).[65] Based on this work, we expected that PDMAEMA and/or q-PDMAEMA films could be used for formation of abiological inorganic thin films in the presence of properly chosen precursors that substitute for silicic acid derivatives. We chose titanium bis(ammonium lactato)dihydroxide (TBALDH) as a precursor of TiO_2, because the compound is stable and soluble in water, and has mainly been used as a TiO_2 precursor for the biomimetic formation of TiO_2.[14,42–44] TBALDH has also been used as a TiO_2 source in the processes of thermal[60] and acid decomposition.[64]

Formation of TiO_2/PDMAEMA Films in Aqueous Solutions

We first used PDMAEMA films as a catalytic platform for TiO_2 formation, simply because PDMAEMA acted as an efficient platform for SiO_2 formation in our and others' previous reports.[40,41,66,67] Formation of TiO_2/PDMAEMA thin films was carried out by placing a PDMAEMA-coated substrate in 1 mL aqueous solution (pH 6.7) of TBALDH (50 mM) for 1 h at room temperature.

The presence of TiO_2 species in the resulting films was confirmed by X-ray photoelectron spectroscopy (XPS) and IR spectroscopy. Figure 1 shows the XPS spectra of
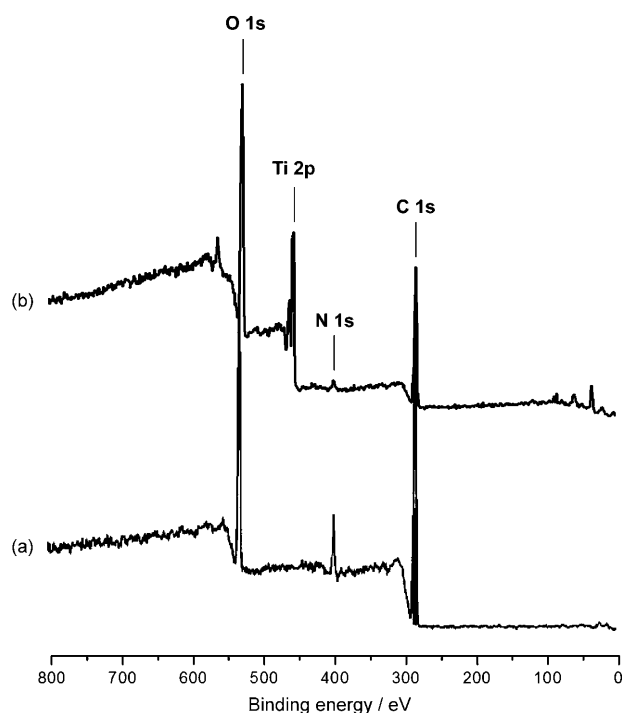
Figure 1. XPS spectra of a) the PDMAEMA film and b) the TiO$_2$/PDMAEMA film. TiO$_2$ was formed in an aqueous solution of TBALDH (50 mM).

PDMAEMA and TiO$_2$/PDMAEMA films. A Ti 2p peak appeared at 458 eV (Figure 1b), in addition to the peaks of O 1s (531 eV), N 1s (402 eV), and C 1s (287 eV) observed from PDMAEMA (Figure 1a). The IR spectrum of the PDMAEMA film showed characteristic peaks at 1732 (C=O stretching), 1461 (-CH$_2$- bending), and 1155 cm^{-1} (C–N stretching; Figure 2a). After the TiO$_2$ formation, a new peak was observed at about 800 cm^{-1} in the IR spectrum.

The peak was rather broad, ranging from 450 to 1000 cm^{-1} (Figure 2b).[68] Although the previous work by others[14,42–44] did not report any IR data of the biomimetically grown TiO$_2$ species, the IR peaks of TiO$_2$ (Ti–O bonds) were reported to appear in the range of 400–1000 cm^{-1}.[69–72] We thought that the observed peak broadening resulted from an amorphous nature of TiO$_2$ thin films that would be caused by incorporation of water and/or carbon species into the Ti–O bond network. Incorporation of water was inferred by the presence of another new peak at 1650 cm^{-1} in Figure 2b (assigned as H$_2$O deformation). In accordance with our inference, when we annealed the substrate at 600°C under N$_2$ for 5 h, the intensity of the peak at 1650 cm^{-1} decreased, and the peak from the Ti–O bond became narrowed and sharpened at 810 cm^{-1} (Figure 2c). The spectroscopic data confirmed that the TiO$_2$/PDMAEMA films were successfully generated in aqueous solution at neural pH (6.7) and room temperature. As control experiments, we formed films of poly(methyl methacrylate) (PMMA) and poly(N-isopropylacrylamide) (PNIPAAm). Neither PMMA nor PNIPAAm induced TiO$_2$ formation.

Surface morphology of the films was investigated by atomic force microscopy (AFM; Figure 3a,b). The PDMAEMA film was noticeably uniform as reported before:[40] The root-mean-square (rms) value of the 140 nm-thick film was 0.45 nm (Figure 3a). After the TiO$_2$ formation, the films became roughened: The rms value increased to 9.59 nm, and 100 nm-sized lumps were also observed (Figure 3b). The field-emission scanning electron microscopy (FE-SEM) micrographs also confirmed the presence of TiO$_2$ films (Figure 3c–e). In the cross-sectional views, we observed that the thickness of the TiO$_2$/PDMAEMA film increased to 230 nm (from the 140 nm-thick PDMAEMA film), and the film became rougher after TiO$_2$ formation (Figure 3c,d). The top
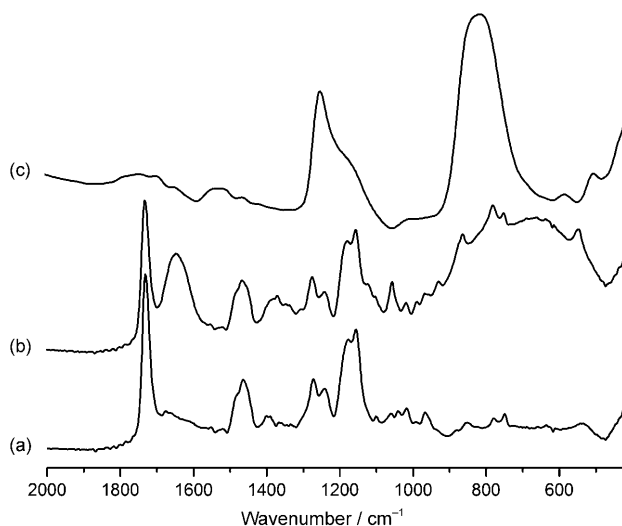

Figure 2. IR spectra of a) the PDMAEMA film, b) the TiO$_2$/PDMAEMA film, and c) the TiO$_2$/PDMAEMA film after annealing. TiO$_2$ was formed in an aqueous solution of TBALDH (50 mM).
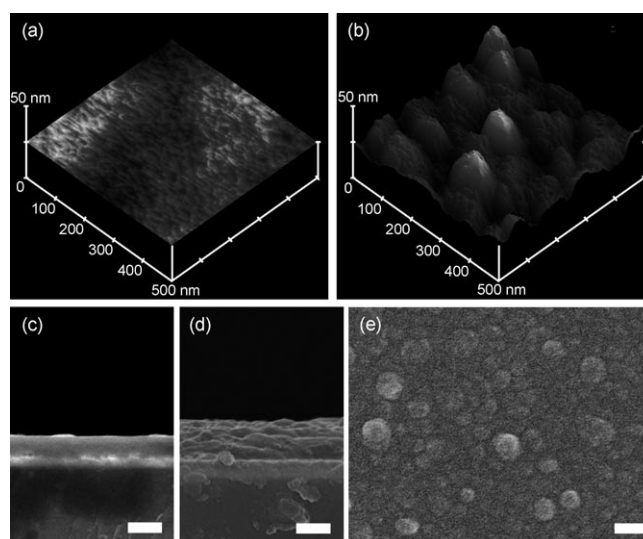

Figure 3. AFM micrographs of a) the PDMAEMA film and b) the TiO$_2$/PDMAEMA film. SEM micrographs of c) the PDMAEMA film (cross-sectional view), d) the TiO$_2$/PDMAEMA film (cross-sectional view), and e) the TiO$_2$/PDMAEMA film (top view). TiO$_2$ was formed in an aqueous solution of TBALDH (50 mM). Scale bar: 200 nm.

view showed that the surface of the TiO$_2$/PDMAEMA film was relatively uniform over the entire area imaged, although composed of lumps (Figure 3e). The indistinguishable layer of PDMAEMA and TiO$_2$ would be evidence for carbon incorporation into the Ti–O bond network. The hybrid nature of the inorganic materials and organic polymers is in agreement with previous reports on the biomimetic formation of silica and TiO$_2$.[38, 40, 44]

Formation of TiO$_2$/PDMAEMA Films in Phosphate-Buffered Solutions

It is well-known that the pH values of reaction media affect processes of biomimetic silicification.[73,74] Briefly, there are the optimal pH ranges for biomimetic silicification, and the size of the precipitated silica spheres strongly depends on pH. We studied the pH effect on TiO$_2$ formation in our system by controlling the acidity of the reaction solutions with phosphate buffer. The employed pH values ranged from 2 to 12 with a single-digit increment. In addition to the pH effect, this experimental setting was also expected to give important information on the participation of anions (phosphates) in the biomimetic processes.

The IR spectra of the resulting samples formed at pH 5 and 10 are shown as representatives in Figure 4. We found that the TiO$_2$ films contained a considerable amount of phosphate anions when formed in the pH range 2–6. For example, when we performed the reaction at pH 5, the resulting TiO$_2$ films showed a strong peak at 1063 cm^{-1} assigned as a PO$_4^{3-}$ out-of-phase stretch, in addition to the broad peak at about 800 cm^{-1} resulting from Ti–O bonds in amorphous TiO$_2$ (Figure 4a).[75,76] We did not observe this peak when the TiO$_2$ formation was performed in aqueous solution (Figure 2b). In the XPS spectrum, the peak corresponding to P 2p was observed at 135 eV (see the Supporting Information, Figure S1a). In contrast, the IR peak for phosphate anions was not observed when the reactions were performed in the pH range 7–12 (Figure 4b), although a weak peak of the incorporated phosphate ions could be detected
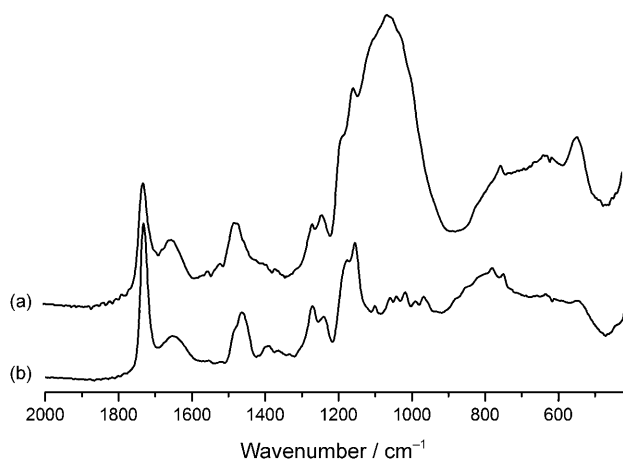

Figure 4. IR spectra of the TiO$_2$/PDMAEMA films formed in the phosphate-buffered solutions: a) pH 5, b) pH 10.

in the XPS spectra (Figure S1b in the Supporting Information). The results indicate that phosphate anions were incorporated into the TiO$_2$/PDMAEMA films to a lesser extent under basic conditions (at high pH). Connor et al. reported that phosphate anions were strongly adsorbed onto TiO$_2$ films at low pH, but not at high pH, which is in agreement with our results.[75] The observed pH dependency of phosphate adsorption could be reasoned by competitive adsorption of hydroxide (OH$^-$) at high pH.[77,78] Another possibility would be pre-association of phosphate anions with PDMAEMA. Because the pK_a values of phosphoric acid are about 2.12 (pK_{a1}), 7.21 (pK_{a2}), and 12.67 (pK_{a3}), H$_2$PO$_4^-$ and HPO$_4^{2-}$ predominantly exist in the phosphate-buffered solutions (pH 2–12). The pK_a value of PDMAEMA is about 8,[79] and therefore a high portion of 2-(dimethylamino)ethyl chains are protonated in the range of pH 2–6 and could make a complex with phosphate anions. Owing to deprotonation (or nonprotonation), 2-(dimethylamino)ethyl groups are neutral at high pH value and presumably do not have much tendency to associate with phosphate anions.

The presence of the phosphate anions did not alter the broad IR peak at about 800 cm^{-1} in the pH values studied, which means that the pH value did not affect the formation of TiO$_2$ thin films except for the adsorption of phosphate anions in the phosphate-buffered solutions. In other words, the formation of TiO$_2$ films occurred in all the pH values of phosphate-buffered solutions studied (pH 2–12),[44] with different chemical compositions and perhaps structures. It remains to be seen how the pH values and the incorporation of phosphate anions affect the reaction pathways (and mechanisms) of TiO$_2$ film formation.

Crystallization of TiO$_2$

We did not observe any characteristic peaks for crystal structures of TiO$_2$ in the X-ray diffraction (XRD) spectra, indicative of the amorphous nature of the formed TiO$_2$ films (Figure 5a). The XRD data agreed well with the broad IR peak described above. We attempted the conversion of amorphous TiO$_2$ to anatase or rutile phase by annealing the TiO$_2$/PDMAEMA film, which had been formed in the aqueous solution without phosphate anions, at 600°C under N$_2$ for 5 h. After annealing, we observed a new peak at 25.3° (2Θ) in the XRD spectrum (Figure 5b), in addition to strong peaks from Au at 38.3° (111) and 44.7° (200) (for wide-ranged XRD spectra, see Figure S2 in the Supporting Information). The peak is one of the characteristic peaks for the anatase phase, which is the dominant crystal structure of TiO$_2$. The other peaks from anatase were concealed by the strong peaks from Au (Figure S2 in the Supporting Information).

While phosphate anions did not affect the TiO$_2$ film formation itself, it was found to affect the crystallization processes of TiO$_2$ in our system. The XRD peak at 25.3°, indicative of the anatase phase, became relatively diminished for the sample that had been generated at pH 10 (Figure 5c), and nearly unobservable for the sample at pH 5
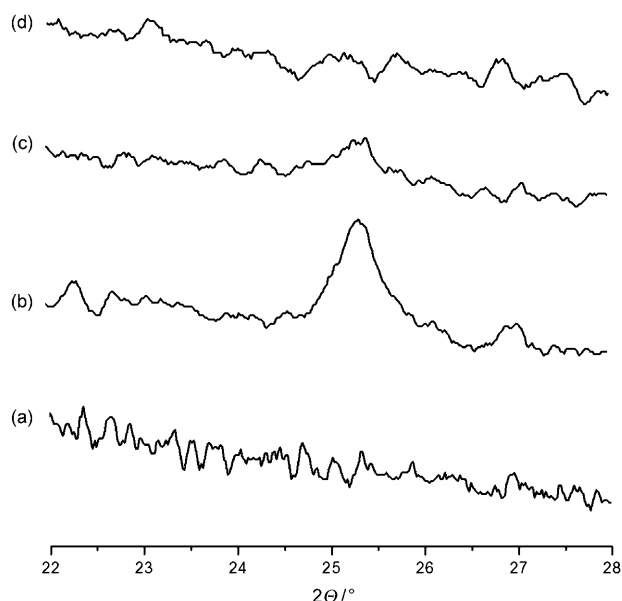
Figure 5. XRD spectra of the TiO₂/PDMAEMA films formed in an aqueous solution of TBALDH (50 mM): a) before annealing, b) after annealing. XRD spectra of the TiO₂/PDMAEMA films formed in the phosphate-buffered solutions, after annealing: c) pH 10, d) pH 5.

(Figure 5 d). The inhibitory effect of phosphate anions on TiO₂ crystallization has previously been reported:[43,78,80] Phosphate anions inhibit the transitions both from amorphous to anatase phase and from anatase to rutile phase, because phosphate anions that are incorporated into the crystal lattice make it difficult for oxygen atoms to move freely for the phase transition. The IR spectra (Figure 4) indicate that the amount of adsorbed phosphate anions at pH 5 was higher than that at pH 10. Therefore, the transition from amorphous to anatase phase was inhibited more at pH 5 than at pH 10 in our system.

The chemical nature of TiO₂ before and after annealing was further characterized by the deconvoluted XPS spectra. Before annealing, the XPS peaks from Ti 2p$_{1/2}$ and Ti 2p$_{3/2}$ were observed at 464.5 and 458.8 eV, in a good agreement with the reported values for TiO₂ (Ti^{4+}; Figure 6 a).[81,82] The O 1s peaks were deconvoluted to 529.3, 530.6, 531.7, and 533.5 eV (Figure 6 b): The peak at 529.3 eV was assigned as oxygen in the TiO₂ lattice and the peak at 530.6 eV as dangling oxygen (OH). The two remaining peaks

(at 531.7 and 533.5 eV) were thought to come from oxygen atoms of PDMAEMA, because the XPS spectrum of the PDMAEMA film showed peaks at 529.8, 531.8, and 533.4 eV before TiO₂ deposition. Along with the XRD spectrum (Figure 5 a), the XPS spectra indicated the formation of amorphous TiO₂.[83] The O/Ti ratio was calculated to be about 2.01, based on the O 1s peaks only at 529.3 and 530.6 eV and the Ti 2p peaks with their atomic sensitivity factors (0.66 and 1.8).[84] The XPS characterization corresponded well with the hybrid nature of inorganic materials and polymers in biomimetic processes. After annealing, the peak positions for Ti were shifted slightly to 464.1 and 458.4 eV (Figure 6 c). Of interest, only two peaks for O 1s were observed at 529.7 and 531.1 eV, which were assigned as oxygen in the TiO₂ lattice and dangling oxygen, respectively. The peaks corresponded with previous reports on anatase crystalline structures on the nanometer scale.[85,86]

Formation of TiO₂/q-PDMAEMA Films

As described in the Introduction, silaffins in diatoms contain modified lysine residues, which are mostly tertiary and quaternary amines. Tertiary amines in silaffins are protonated under physiological conditions, which implies that positively charged amines—protonated tertiary amines and quaternary amines—would play a crucial role in biosilicification in diatoms. We and others have utilized quaternized PDMAEMA and other positively charged amines as a synthetic counterpart of silaffins for biomimetic silicification.[65–67,87] The quaternization of the PDMAEMA film was achieved simply by reaction with bromoethane,[65] and the TiO₂ for-

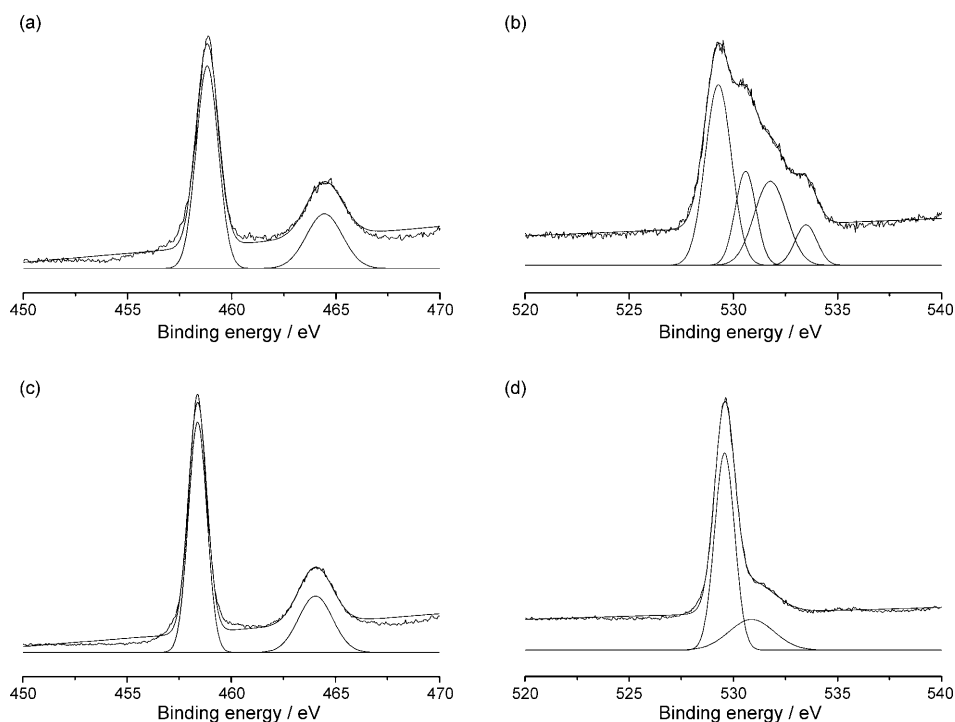Figure 6. Narrow-scanned XPS spectra of the TiO2/PDMAEMA film. a) Ti 2p region before annealing, b) O 1s region before annealing, c) Ti 2p region after annealing, and d) O 1s region after annealing.

mation was performed on the q-PDMAEMA film by following the same procedure as that for the PDMAEMA film (50 mM TBALDH, 1 h at room temperature). The q-PDMAEMA film also acted as a catalytic platform for the biomimetic TiO_2 formation at surfaces. The IR spectrum of the TiO_2/q-PDMAEMA film showed a broad peak in the range of 450 to 1000 cm^{-1} with a maximum at 780 cm^{-1}. The relative intensity of the peak, however, was much higher than that for the TiO_2/PDMAEMA film (Figure 7a, bottom spectrum), which indicates that the relative amount of deposited TiO_2 was greater on the q-PDMAEMA film than on the PDMAEMA film.[88] After annealing the TiO_2/q-PDMEAMA film, we observed the same trend in the IR spectrum as the TiO_2/PDMAEMA film (Figure 7a, top spectrum). Other characteristics, such as pH dependency and incorporation of phosphate anions, were also the same (Figures S3 and S4 in the Supporting Information). q-PDMAEMA is intrinsically positively charged, which means that q-PDMAEMA, in principle, could complex with phosphate anions in the entire range of pH (pH 2–12). The observed pH dependency of phosphate incorporation, therefore, would support the association of phosphate anions with TiO_2 and competitive adsorption of hydroxide at least in the case of q-PDMAEMA.

The AFM micrograph of the TiO_2/q-PDMAEMA film showed more heterogenized and increased roughness compared with the TiO_2/PDMAEMA film: The rms value increased from 0.67 to 21.01 nm (Figure 7b). This increase in the roughness was much greater than that for the PDMAEMA film (0.45 to 9.59 nm). The SEM micrographs also showed the highly roughened TiO_2/q-PDMAEMA film. The q-PDMAEMA film was quite uniform, and the thickness was measured to be about 200 nm (Figure 7c). In contrast, the TiO_2/q-PDMAEMA film was too rough to measure the

exact thickness in the SEM micrographs, and the thickness was only estimated to be 300 nm at the minimum (Figure 6d). In addition, the structure was much more disordered than the TiO_2/PDMAEMA film (Figure 7e). To the best of our knowledge, similarities and differences of tertiary and quaternary amines in biomimetic TiO_2 formation have not been investigated in detail. As a related work, Armes et al. have reported that quaternization of PDMAEMA affected the processes of silica formation in solution, although the exact reason or mechanism was unclear because of various competing factors, such as accessibility of silicic acid and catalytic efficiency of cationic chains.[66,67] They found that quaternization of PDMAEMA was beneficial for producing thicker silica shells as well as controlling silica deposition.[67] In addition, our previous report also showed thicker and rougher SiO_2 films from the q-PDMAEMA film.[65] Taken together, it is concluded that the use of q-PDMAEMA led to the formation of thicker films of SiO_2 and TiO_2 in a somewhat uncontrollable way; it is beneficial in the formation of thick silica shells, but not for the formation of uniformly deposited TiO_2 films. In the case of TiO_2 films, the overall uniformity in thickness and morphology is more important than the amount of deposition. It can be inferred that the quaternization of PDMAEMA resulted in the increased ability of complexing with TiO_2 precursors and inducing TiO_2 formation. However, as seen often in nature, structural optimization is not always directed by the highest efficiency. There would be an optimal condition for biomineralization in the aspect of the degree of quaternization (charge development), anion complexation, and deposition efficiency, which is our next research thrust.

Conclusions

The extreme synthetic conditions of some inorganic materials have limited potentially synergistic combination of inorganic materials and biological entities, and subsequent applications. As an alternative to the chemical method, the biomimetic approach has been attempted to expand the range of applications of inorganic materials. In this paper, we reported the formation of abiological TiO_2 thin films under ambient conditions by using PDMAEMA and q-PDMAEMA as biomimetic templates. This report is the first example of biomimetic formation of abiological inorganic thin films at neutral pH and room temperature by using tertiary and quaternary amine-containing polymers, and suggests that biosilicification processes found in diatoms could be applied to the fabrication of thin films of various abiological metal oxides, such as titanium oxide, gallium oxide, and germanium oxide.

We found that there were no optimal pH ranges for biomimetic TiO_2 formation at surfaces in phosphate-buffered solutions; TiO_2 thin films were formed in the entire pH range employed (pH 2 to 12). The chemical composition of the composite layers was, however, found to be dependent upon pH. Phosphates were incorporated into the composite
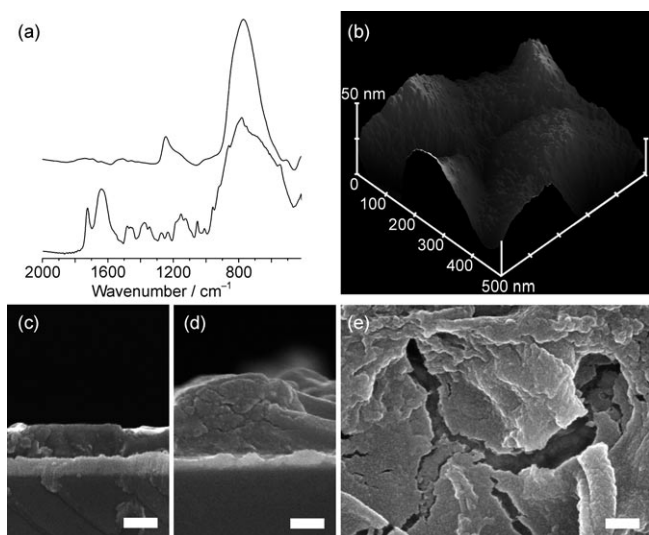

Figure 7. a) IR spectra of the TiO_2/q-PDMAEMA film before (bottom) and after annealing (top). b) AFM micrograph of the TiO_2/q-PDMAEMA film. SEM micrographs of c) the q-PDMAEMA film (cross-sectional view), d) the TiO_2/q-PDMAEMA film (cross-sectional view), and e) the TiO_2/q-PDMAEMA film (top view).

layers under acidic conditions, but the incorporation became less as the pH values were increased. The morphological variation of the composite films was also achieved by the quaternization of PDMEMA films.

Experimental Section

Materials

2-(Dimethylamino)ethyl methacrylate (DMAEMA, 98%, Sigma–Aldrich), copper(I) bromide (CuBr, 99.999%, Sigma–Aldrich), 2,2′-dipyridyl ($\geq$99%, Sigma–Aldrich), bromoethane (C_2H_5Br, 99+%, Sigma–Aldrich), bis(ammonium lactato)dihydroxide (50 wt% solution in water, Sigma–Aldrich), aluminum oxide (Al_2O_3, activated, basic, Brockmann I, standard grade, 150 mesh, Sigma–Aldrich), nitromethane (CH_3NO_2, 96%, Sigma–Aldrich), and absolute ethanol (99.8%, Merck) were used as received. Ultrapure water (18.3 MΩ cm) from the Human Ultrapure System (Human Corp., Korea) was used. The polymerization initiator $BrC(CH_3)_2COO(CH_2)_{11}S)_2$ was synthesized by following the reported procedure.[89]

Formation of PDMAEMA and Quaternized PDMAEMA Films

The self-assembled monolayers (SAMs) of the polymerization initiator were formed by immersing a gold-coated silicon wafer in a 1 mM ethanol solution of $(BrC(CH_3)_2COO(CH_2)_{11}S)_2$ for 24 h at room temperature. After formation of the SAMs, the gold substrate was rinsed with ethanol several times and then was dried under a stream of argon. The formation of the SAMs was confirmed by polarized infrared external reflectance spectroscopy: 1737 (C=O stretching), 1465 (-CH$_2$- bending), and 1169 cm^{-1} (C–O stretching). Before performing surface-initiated, atom transfer radical polymerization (SI-ATRP) of DMAEMA, DMAEMA was purified by column chromatography on basic aluminum oxide, and water was degassed and purged with argon. All the polymerization steps were carried out in argon atmosphere. The initiator-coated gold substrate (4×6 cm^2) was placed in a reaction mixture of degassed water (60 mL), purified DMAEMA (60 mmol), CuBr (0.6 mmol), and 2,2′-dipyridyl (1.2 mmol). The resulting mixture was kept without stirring for 4 h at room temperature, and then the PDMAEMA-coated gold substrate was taken, rinsed with water and ethanol, and dried under a stream of argon. The formation of the PDMAEMA film was confirmed by a previously reported method.[40] Briefly, the IR spectrum of PDMAEMA (140 nm in thickness by ellipsometric measurement) showed peaks at 1732 (C=O stretching), 1461 (-CH$_2$- bending), and 1155 cm^{-1} (C–N stretching). On the other hand, quaternization of the PDMAEMA film was performed by placing a PDMAEMA-coated substrate (4×3 cm^2) in the mixture of bromoethane (10 mL) and nitromethane (10 mL) for 12 h at room temperature.[65] The substrate was taken, rinsed with dichloromethane and ethanol, and finally dried under a stream of argon. The formation of quaternized PDMAEMA (q-PDMAEMA) was confirmed by ellipsometry and contact-angle measurement. The ellipsometric thickness of the q-PDMAEMA film increased to 200 nm (from the 140 nm-thick PDMAEMA film). The water contact angle of the PDMAEMA film was 53°, but that of the q-PDMAEMA film was reduced to 38°.

Biomimetic Formation of TiO_2 Films

The substrates coated with PDMAEMA or q-PDMAEMA were cut into pieces (ca. 1×0.5 cm^2), and a piece was placed in 50 mM aqueous solution of titanium bis(ammonium lactato)dihydroxide (TBALDH; 1 mL). After 1 h at room temperature, the substrate was rinsed with water several times and dried under a stream of argon. To investigate the pH effect on TiO_2 formation, the substrates were placed in a 1 mL aqueous mixture of phosphate buffer (50 mM, various pH values) and TBALDH (50 mM) for 1 h at room temperature.

Characterization

The thickness of monolayers and polymeric films was measured with a Gaertner L116s ellipsometer (Gaertner Scientific Corporation, IL)

equipped with a He–Ne laser (632.8 nm) at a 70° angle of incidence. A refractive index of 1.46 was used for all the films. The X-ray photoelectron spectroscopy was performed with a VG-Scientific ESCALAB 250 spectrometer (United Kingdom) with a monochromatized Al K$_\alpha$ X-ray source (1486.6 eV). Emitted photoelectrons were detected by a multichannel detector at a takeoff angle of 90° relative to the surface. During the measurements, the base pressure was 10^{-9}–10^{-10} Torr. Survey spectra were obtained at a resolution of 1 eV from one scan, and high-resolution spectra were acquired at a resolution of 0.05 eV from five scans. Infrared spectra were obtained with an IFS66 V/S (Bruker Optiks, Germany) at an 80° angle of incidence. Atomic force microscopy imaging was performed in a tapping mode on a Nanoscope IIIa multimode scanning probe microscope (Veeco, United States) with a tapping mode etched silicon probe. Field-emission scanning electron microscopy micrographs were obtained with Sirion (FEI Co., Netherlands) after platinum coating. Crystal phases of TiO_2 films were characterized with a D/MAX-2500 (18 kW) multipurpose attachment X-ray diffractometer (Rigaku, Japan).

[1] C. N. R. Rao, B. Raveau, *Transition Metal Oxides: Structure, Properties, and Synthesis of Ceramic Oxides, 2nd ed.*, Wiley, New York, **1998**.

[2] C. C. Koch, *Nanostructured Materials*, William Andrew, Norwich, **2002**.

[3] H. A. Lowenstam, *Science* **1981**, *211*, 1126.

[4] M. Sumper, *Angew. Chem.* **2004**, *116*, 2301; *Angew. Chem. Int. Ed.* **2004**, *43*, 2251.

[5] L. L. Brott, R. R. Naik, D. J. Pikas, S. M. Kirkpatrick, D. W. Tomlin, P. W. Whitlock, S. J. Clarson, M. O. Stone, *Nature* **2001**, *413*, 291.

[6] H. A. Lowenstam, S. Weiner, *On Biomineralization*, Oxford University, Oxford, **1989**.

[7] F. C. Meldrum, *Inter. Mater. Rev.* **2003**, *48*, 187.

[8] M. Sumper, N. Kröger, *J. Mater. Chem.* **2004**, *14*, 2059.

[9] R. Blackmore, *Science* **1975**, *190*, 377.

[10] P. M. Harrison, A. Treffry, T. H. Lilley, *J. Inorg. Biochem.* **1986**, *27*, 287.

[11] T. Douglas, V. T. Stark, *Inorg. Chem.* **2000**, *39*, 1828.

[12] M. Okuda, K. Iwahori, I. Yamashita, H. Yoshimura, *Biotechnol. Bioeng.* **2003**, *84*, 187.

[13] H. A. Hosein, D. R. Strongin, M. Allen, T. Douglas, *Langmuir* **2004**, *20*, 10283.

[14] J. L. Sumerel, W. Yang, D. Kisailus, J. C. Weaver, J. H. Choi, D. E. Morse, *Chem. Mater.* **2003**, *15*, 4804.

[15] D. Kisailus, J. H. Choi, J. C. Weaver, W. Yang, D. E. Morse, *Adv. Mater.* **2005**, *17*, 314.

[16] S. V. Patwardhan, S. Clarson, *J. Polymer* **2005**, *46*, 4474.

[17] M. Allen, D. Willits, M. Young, T. Douglas, *Inorg. Chem.* **2003**, *42*, 6300.

[18] C. E. Flynn, C. Mao, A. Hayhurst, J. L. Williams, G. Georgiou, B. Iverson, A. M. Belcher, *J. Mater. Chem.* **2003**, *13*, 2414.

[19] M. B. Dickerson, R. R. Naik, M. O. Stone, Y. Cai, K. H. Sandhage, *Chem. Commun.* **2004**, 1776.

[20] J. N. Cha, K. Shimizu, Y. Zhou, S. C. Christiansen, B. F. Chemelka, G. D. Stucky, D. E. Morse, *Proc. Natl. Acad. Sci. USA* **1999**, *96*, 361.

[21] F. E. Round, R. M. Crawford, D. G. Mann, *The Diatoms: Biology & Morphology of the Genera*, Cambridge University, Cambridge, **1990**.

[22] V. C. Sundar, A. D. Yablon, J. L. Grazul, M. Ilan, J. Aizenberg, *Nature* **2003**, *424*, 899.

[23] M. Sumper, *Science* **2002**, *295*, 2430.

[24] N. Kröger, S. Lorenz, E. Brunner, M. Sumper, *Science* **2002**, *298*, 584.

[25] F. Noll, M. Sumper, N. Hampp, *Nano Lett.* **2002**, *2*, 91.

[26] M. R. Knecht, D. W. Wright, *Chem. Commun.* **2003**, 3038.

[27] N. Kröger, R. Deutzmann, M. Sumper, *J. Biol. Chem.* **2001**, *276*, 26066.

[28] N. Kröger, R. Deutzmann, C. Bergsdorf, M. Sumper, *Proc. Natl. Acad. Sci. USA* **2000**, *97*, 14133.

[29] M. Sumper, S. Lerenz, E. Brunner, *Angew. Chem.* **2003**, *115*, 5350; *Angew. Chem. Int. Ed.* **2003**, *42*, 5192.

[30] M. Sumper, N. Kröger, *J. Mater. Chem.* **2004**, *14*, 2059.

[31] S. V. Patwardhan, N. Mukherjee, S. J. Clarson, *J. Inorg. Organomet. Polym.* **2001**, *11*, 193.

[32] S. V. Patwardhan, S. J. Clarson, *J. Inorg. Organomet. Polym.* **2003**, *13*, 49.

[33] S. V. Patwardhan, S. J. Clarson, *J. Inorg. Organomet. Polym.* **2003**, *13*, 193.

[34] S. V. Patwardhan, N. Mukherjee, S. Clarson, *J. Silicon Chem.* **2002**, *1*, 47.

[35] S. V. Patwardhan, N. Mukherjee, S. J. Clarson, *J. Inorg. Organomet. Polym.* **2001**, *11*, 117.

[36] E. Brunner, K. Lutz, M. Sumper, *Phys. Chem. Chem. Phys.* **2004**, *6*, 854.

[37] S. V. Patwardhan, S. Clarson, *J. Mater. Sci. Eng.* **2003**, *23*, 495.

[38] M. R. Knecht, D. W. Wright, *Langmuir* **2004**, *20*, 4728.

[39] S. V. Patwardhan, S. Clarson, *J. Silicon Chem.* **2002**, *1*, 207.

[40] D. J. Kim, K.-B. Lee, Y. S. Chi, W. J. Kim, H.-j. Paik, I. S. Choi, *Langmuir* **2004**, *20*, 7904.

[41] D. J. Kim, K.-B. Lee, T. G. Lee, H. K. Shon, W.-J. Kim, H.-j. Paik, I. S. Choi, *Small* **2005**, *1*, 992.

[42] M. J. Pender, L. A. Sowards, J. D. Hartgerink, M. O. Stone, R. R. Naik, *Nano Lett.* **2006**, *6*, 40.

[43] S. L. Sewell, D. W. Wright, *Chem. Mater.* **2006**, *18*, 3108.

[44] N. Kröger, M. B. Dickerson, G. Ahmad, Y. Cai, M. S. Haluska, K. H. Sandhage, N. Poulsen, V. C. Sheppard, *Angew. Chem.* **2006**, *118*, 7397; *Angew. Chem. Int. Ed.* **2006**, *45*, 7239.

[45] It should be noted that in these reports, references [14,42–44], the same precursor of TiO$_2$, titanium bis(ammonium lactate)dihydroxide, was used for biomimetic formation of titania based on the work by Morse and co-workers.[14]

[46] T. Watanabe, A. Kitamura, E. Kojima, C. Nakayama, K. Hashimoto, A. Fujishima, *Photocatalytic Purification and Treatment of Water and Air*, Elsevier, Amsterdam, **1993**, pp. 747–751.

[47] A. Fujishima, K. Honda, *Nature* **1972**, *238*, 37.

[48] M. Grätzel, *Comments Inorg. Chem.* **1991**, *12*, 93.

[49] T. Fujii, N. Sakata, J. Takada, Y. Miura, Y. Daitoh, *J. Mater. Res.* **1994**, *9*, 1468.

[50] G. A. Battiston, R. Gerbasi, M. Porchia, A. Marigo, *Thin Solid Films* **1994**, *239*, 186.

[51] L. M. Williams, D. W. Hess, *J. Vac. Sci. Technol. A* **1983**, *1*, 1810.

[52] H. Tang, K. Prasad, R. Sanjinès, P. E. Schmid, F. Lévy, *J. Appl. Phys.* **1994**, *75*, 2042.

[53] S. Ben Amor, G. Baud, J. P. Besse, M. Jacqet, *Thin Solid Films* **1997**, *293*, 163.

[54] N. Martin, C. Rousselot, D. Rondot, F. Palmino, R. Mercier, *Thin Solid Films* **1997**, *300*, 113.

[55] S. Takeda, S. Suzuki, H. Odaka, H. Hosono, *Thin Solid Films* **2001**, *392*, 338.

[56] M. Gilo, N. Croitoru, *Thin Solid Films* **1996**, *283*, 84.

[57] T. Watanabe, A. Kitamura, E. Kojima, C. Nakayama, K. Z. Hashimoto, A. Fujishima, *Chem. Lett.* **1994**, 723.

[58] A. Wold, *Chem. Mater.* **1993**, *5*, 280.

[59] T. J. Trentler, T. E. Denler, J. F. Bertone, A. Agrawal, V. L. Colvin, *J. Am. Chem. Soc.* **1999**, *121*, 1613.

[60] H. Möckel, M. Giersig, F. Willig, *J. Mater. Chem.* **1999**, *9*, 3051.

[61] H. Shin, R. J. Collins, M. R. DeGuire, A. H. Heuer, C. N. Sukenik, *J. Mater. Res.* **1995**, *10*, 692.

[62] H. Shin, R. J. Collins, M. R. DeGuire, A. H. Heuer, C. N. Sukenik, *J. Mater. Res.* **1995**, *10*, 699.

[63] Y.-F. Gao, Y. Masuda, K. Koumoto, *Chem. Mater.* **2004**, *16*, 1062, and references therein.

[64] S. Baskaran, L. Song, J. Liu, Y. L. Chen, G. L. Graff, *J. Am. Ceram. Soc.* **1998**, *81*, 401.

[65] W. K. Cho, S. M. Kang, D. J. Kim, S. H. Yang, I. S. Choi, *Langmuir* **2006**, *22*, 11208.

[66] Y. Jia, G. M. Gray, J. N. Hay, Y. Li, G.-F. Unali, F. L. Baines, S. P. Armes, *J. Mater. Chem.* **2005**, *15*, 2202.

[67] J. J. Yuan, O. O. Mykhaylyk, A. J. Ryan, S. P. Armes, *J. Am. Chem. Soc.* **2007**, *129*, 1717.

[68] In Figure 2b, we also observed very weak IR peaks from organic species (PDMAEMA and/or ligands of TBALDH) at 1370 (CH$_3$ symmetric deformation) and 1055 cm^{-1} (C–O stretching) but could not clearly identify IR peaks from the ligands of TBALDH. We, however, did not exclude the possibility of the incorporation of the ligands into the TiO$_2$/PDMAEMA film.

[69] H. Li, C. P. Tripp, *Langmuir* **2005**, *21*, 2585.

[70] W. G. Lee, S. I. Wo, J. C. Kim, S. H. Choi, K. H. Oh, *Thin Solid Films* **1994**, *237*, 105.

[71] M. L. Calzada, L. Del Olmo, *J. Non-Cryst. Solids* **1990**, *121*, 413.

[72] T. Kamada, M. Kitagawa, M. Shibuya, T. Hirao, *Jpn. J. Appl. Phys.* **1991**, *30*, 3594.

[73] H. Menzel, S. Horstmann, P. Behrens, P. Bärnreuther, I. Krueger, M. Jahns, *Chem. Commun.* **2003**, 2994.

[74] K. Lutz, C. Grögger, M. Sumper, E. Brunner, *Phys. Chem. Chem. Phys.* **2005**, 7, 2812.

[75] P. A. Connor, A. McQuillan, *Langmuir* **1999**, *15*, 2916.

[76] M. I. Tejedor-Tejedor, M. A. Anderson, *Langmuir* **1990**, *6*, 602.

[77] H. P. Böehm, *Adv. Catal.* **1966**, *16*, 179.

[78] J. Criado, C. Real, *J. Chem. Soc. Faraday Trans. 1* **1983**, *79*, 2765.

[79] M. J. Bruining, H. G. T. Blaauwgeers, R. Kuijer, E. Pels, R. M. M. A. Nuijts, L. H. Koole, *Biomaterials* **2000**, *21*, 595.

[80] J. C. Yu, L. Zhang, Z. Zheng, J. Zhao, *Chem. Mater.* **2003**, *15*, 2280.

[81] C. N. Sayers, N. R. Armstrong, *Surf. Sci.* **1978**, *77*, 301.

[82] D.-J. Won, C.-H. Wang, H.-K. Jand, D.-J. Choi, *Appl. Phys. A*, **2001**, *73*, 595.

[83] Z. Zhao, B. K. Tay, G. Yu, *Appl. Optics* **2004**, *43*, 1281.

[84] C. D. Wagner, L. E. Davis, M. V. Zeller, J. A. Taylor, R. M. Raymond, L. H. Gale, *Surf. Interface Anal.* **1981**, *3*, 211.

[85] L. Wu, J. C. Yu, X. C. Wang, L. Zhang, J. Yu, *J. Solid State Chem.* **2005**, *178*, 321.

[86] V. H. Grassian, P. T. O'Shaughnessy, A. Adamcakova-Dodd, J. M. Pettibone, P. S. Thorne, *Environmental Health Perspectives* **2007**, *115*, 397.

[87] G. M. Gray, J. N. Hay, *Mater. Res. Soc. Symp. Proc.* **2003**, *775*, 179.

[88] We additionally formed two new films of amine-containing polymers, poly(aminoethyl methacrylate) (PAEMA) and poly(2-(*tert*-butylamino)ethyl methacrylate) (PTBAEMA). The former contained primary amines and the later contained secondary amines. The IR and SEM characterizations indicated that these two polymeric films also induced the TiO$_2$ deposition, and the resulting films were relatively uniform (see Figures S5 and S6 in the Supporting Information for the SEM micrographs). The only quaternary amine-containing polymer, q-PDMAEMA, led to uncontrollable TiO$_2$ deposition. These results indicated that the chemical nature of positive charges would be more important than methylation in the control of TiO$_2$ deposition. In the case of primary, secondary, and tertiary amines, positive charges, generated by protonation, would not be developed in the entire films of polymers. In contrast, permanent positive charges, present on q-PDMAEMA, could induce TiO$_2$ formation along the whole layer of the q-PDMAEMA film in a somewhat uncontrollable manner.

[89] R. R. Shah, D. Merreceyes, M. Husemann, I. Rees, N. L. Abbott, C. J. Hawker, J. L. Hedrick, *Macromolecules* **2000**, *33*, 597.